Mössbauer studies of bound diffusion in a model polymer system

A. S. Plachinda
Institute of Chemical Physics of the Academy of Sciences of the U.S.S.R., 117977 Moscow, U.S.S.R.

V. E. Sedov*
I. V. Kurchatov Institute of Atomic Energy, 123182 Moscow, U.S.S.R.

V. I. Khromov, I. P. Suzdalev, and V. I. Goldanskii
Institute of Chemical Physics of the Academy of Sciences of the U.S.S.R., 117977 Moscow, U.S.S.R.

G. U. Nienhaus
Department of Physics, University of Illinois at Urbana-Champaign, Urbana, Illinois 61801

F. Parak†
Institut für Molekulare Biophysik der Universität Mainz, Jakob Welder Weg 26, 6500 Mainz, Germany
(Received 23 August 1991)

Iron hydroxide particles with diameters of about 3 nm have been precipitated in a network of polymer chains of sulfonated polystyrene, cross-linked by divinylbenzene. The dynamics of these iron particles has been investigated by Mössbauer spectroscopy. The spectra were analyzed using a generalized Brownian oscillator model, in which the bound diffusion proceeds in an arbitrary potential. Samples with different degrees of cross-linkage have been investigated. The water content of the samples was varied, and the viscosity of the water was increased by the addition of sucrose solution. It can be shown that the size of the cages formed by the polymer chains essentially determines the type of diffusion. If the iron hydroxide particles have no free space, the dynamics is determined by the polymer network. With an increase of the free volume, the iron hydroxide particles show the typical behavior of bound diffusion in a hard cage. By increasing the size of the cage further, one attains a situation close to free diffusion. Varying the viscosity of the solvated liquid in a sample with a given cage size leads to a dynamics of the iron hydroxide particles that shows the expected dependence on the diffusion constant D. It should be noted that some of the samples show unusually broad Mössbauer spectra, with a half width up to 500 mm/s.

INTRODUCTION

It has been known for a long time that the Mössbauer effect is a good tool in the study of slow motions.[1] The conclusions of the general theory have been confirmed in the most evident case of free diffusion of small particles in viscous liquids as well as of diffusion of impurities in crystals. The dynamics results in a broadening of the Mössbauer line without any loss of area. The diffusion coefficient can be derived from the linewidth.[2–4] On the other hand, when the possible positions of a Mössbauer probe are limited in space the spectra should consist of a set of Lorentzians with different widths and intensities.[5] The jumping of atoms among a few discrete sites has been analyzed in the studies of interstitials and hydrogen in metals.[6–9]

In recent years, special attention has been paid to the dynamics of proteins and synthetic polymers. In biopolymers, a strong correlation exists between the intramolecular mobility and the functional activity. Mössbauer absorption spectroscopy provides information on the modes of motions coupled to the iron.[10–15] Rayleigh scattering of Mössbauer radiation (RSMR) makes it possible to separate segmental motions within proteins as well as intermolecular long-range correlated motions.[16–18] For a review of further literature on mobility and diffusion, we refer to Refs. 19 and 20. A lot of Mössbauer data have been accumulated. Nevertheless, there remain problems of interpretation. The motion of a given part of the molecule consists of many modes corresponding to numerous degrees of freedom of the macromolecular system. Hence the Mössbauer spectra carry an abundance of information which cannot be unambiguously extracted from experimental data. One is forced to use reliable methods to visualize the simplest features of behavior of the probe. For it is not possible to start from the first principles of quantum mechanics; the dynamics of Mössbauer nuclei should be described by a theoretical model introduced *ab initio*.

In several investigations of proteins, the model of a single (or many coupled) overdamped Brownian oscillator(s) has been used successfully.[13–15,21] A few years ago a concept was proposed that generalized the Brownian oscillator model.[22,23] In this approach the bound diffusion proceeds in an arbitrary potential $U(\mathbf{r})$, and the harmonic Brownian oscillator appears to be a special case of this.

It was shown that the Mössbauer spectra can be surprisingly sensitive to its profile.[23] In particular, it appeared that the temperature dependence of the weight of the narrow spectral component (Lamb-Mössbauer factor) is directly determined by $U(\mathbf{r})$. In principle, this opens the door to a direct reconstruction of the potential from the Mössbauer data. Due to the typical inversion problem this attractive opportunity seems feasible only for special cases where additional knowledge of the system is available. Therefore, even using these methods of interpretation we need the most simple model systems giving easily tractable results.

In this work we have studied the diffusion of ultrafine particles of ferric hydroxide precipitated inside a polymeric network. These particles are able either to diffuse within the cages formed by the polymer chains or to shift with the whole polymer fragments. In principle, special modes of motions within the particles also have to be taken into account. The particles are large enough so that their motions are a good example of classical bound diffusion. It will be shown how the Mössbauer spectra can be used to reconstruct their motions completely. Preliminary results have been given in Refs. 24–27.

SAMPLE PREPARATION AND EXPERIMENTAL EQUIPMENT

For our investigations, the reactive polymer-cation exchange DOWEX 50W has been used. In this polymer the chains of sulfonated polystyrene are cross-linked by divinylbenzene and form a three-dimensional network. Such a network is able to absorb water in quantities a few times exceeding its initial dry mass. During the preparation, the ferric hydroxide $Fe(OH)_3$ particles, 96.0% enriched with ^{57}Fe, were precipitated inside the polymeric network in the following manner: First, Fe^{3+} ions were introduced into the polymer from sulfate solutions (pH = 1.8) by cation exchange $\underline{3H}^+ + Fe^{3+} \rightleftharpoons \underline{Fe}^{3+} + 3H^+$ amounting to 0.085 g Fe/g dry resin (underlining indicates the exchangeable cations in the resin phase). Then the grains of cation exchanger of the samples, cleaned from surplus liquids, were put into 0.02*M* NaOH. By the reaction $\underline{Fe}^{3+} + 3NaOH \rightleftharpoons \underline{3Na}^+ + Fe(OH)_3$, ultrafine particles of ferric hydroxide were precipitated. It is known that similar particles, precipitated under various conditions, are spherical in shape and always have the same diameter of about 3 nm as observed by means of electron microscopy[28–31] and some other methods, including magnetization measurement[32] and ultracentrifugation.[33] These particles are amorphous[29,31,34,35] and only a very smeared x-ray diffraction pattern is observable.[28,36] As a result only very rough estimates on the oxygen arrangement and ferric ion distributions could be made. Usually it is supposed that their composition is $FeO_{1-x}(OH)_{1+2x}$ $(0 < x < 1)$.[28,37]. The particles are antiferromagnetically ordered. The corresponding hyperfine structure was observed in the Mössbauer spectra at 4.2 K.[28,32,34] All particles show the characteristic transition to the superparamagnetic state, which also makes estimation of their mean radius possible.[38] The temperature dependence of Mössbauer spectra of precipitates in a DOWEX 50 cation

TABLE I. Composition of the different samples.

Sample	1	2	3	4	5	6	7	8	9
Cross-linkage (%)	1	2	2	2	2	4	4	4	12
n	100	50	50	50	50	25	25	25	8
Water content (g water/g polymer)	4.89	3.50	3.50	3.50	3.50	1.92			0.63
^{57}Fe content (mg/cm^2)	4.51	5.10	3.12	3.70	4.48	4.82	8.25	6.85	1.47
Sucrose content (wt%)	60.0	60.0	67.0	63.0	50.0	60.0	43.5	0.0	60.0
Viscosity at 290 K (Ref. 39) (centipoise)	62	62	380	150	21	62	9.3	1.07	62

0.0977

exchanger confirms a particle size of 3 nm. At temperatures above 80 K the magnetic structure is already fully collapsed and the spectra show a pure quadrupole doublet.

In the polymer, the ferric hydroxide particles are immersed into the inner liquid and confined in the cages formed by the polymer chains so that their motions are restricted. The mean cage volume is controlled by preparing samples with different degrees of cross-linkage. In a polymer with 2% cross-linked divinylbenzene, the mean number of elements of the chain between the points of linkage (n) is about 50. Samples with four different degrees of cross-linkage, given in Table I, have been studied. The amount of water as well as the ^{57}Fe content in fully hydrated samples containing particles was strongly dependent on cross-linkage. For comparison a special dried sample without any water was prepared and studied. Since we were mainly interested in the studies of line shapes, samples with decreasing amount of ^{57}Fe content were sometimes used in order to reduce the effective thickness at moderate and low temperatures. For more precise studies of the spectral area at low temperatures an additional sample with natural iron and a cross-linkage of 1% was prepared.

To avoid a phase transition of the solvent in the temperature range under investigation, the water was substituted for a sucrose solution in the final stage of the preparation. The fully hydrated grains of cation exchanger were immersed in the water solution of sucrose for 100–150 h. The final concentration of sucrose was 60 wt %. The volume of the samples remained roughly the same during this procedure. For the studies of the viscosity dependence, we started with sample 6 (compare Table I). From this two different samples, 7 and 8, were prepared and soaked with solutions with various concentrations of sucrose.

A tail cryostat was used to adjust the sample temperatures between 80 and 300 K. The accuracy of the temperature was ±2 K. Mössbauer spectra were obtained using a ^{57}CoRh source, mounted on a special high-velocity drive system which is commercially available. It allows Mössbauer experiments to be carried out with a maximum velocity of 1000 mm/s. Special care had to be taken in order to avoid uncontrolled vibrations of the total equipment. The drive was calibrated at low velocities, using a metallic iron foil. At these velocities the system increased the linewidth by 20%. The high-velocity calibration was obtained by linear extrapolation from low-velocity measurements. This may result in some inaccuracies of the absolute velocity scale.

RESULTS AND DISCUSSION

Figures 1–3 show the temperature dependence of Mössbauer absorption spectra of the samples 2, 1, and 9, respectively. With increasing temperature the spectra of samples 1 and 2 are rapidly broadened and the wings escape from the observation window. At temperatures from 190 to 290 K we were forced to use unconventionally high velocities. The broadening is especially pronounced for the sample 1 (Fig. 2). Here, even the special high-speed spectrometer was not able to collect the whole Mössbauer spectrum at room temperature. Compared with literature values the obtained spectral widths are extremely high for Mössbauer spectroscopy on ^{57}Fe. The broadening of the spectral shape in the case of sample 9 (Fig. 3) is less spectacular and resembles more the behavior observed in biological samples. At first stage the quadrupole doublet seems to collapse but with increasing temperatures it becomes fully resolved again. The latter fact permits us to neglect a possible rotation of the particles. Also we emphasize that the line broadening was observed only for solvated samples. Here, the total area under the spectra falls rapidly at the temperatures higher than 250 K. This could be due to unresolved very broad lines. Line broadening and decrease of the area with increasing temperature are typical features of Mössbauer spectra of supercooled liquids. For $^{57}Fe^{2+}$ in glycerol, the temperature dependence of the spectra was recently explained with a jump model involving broad distribu-

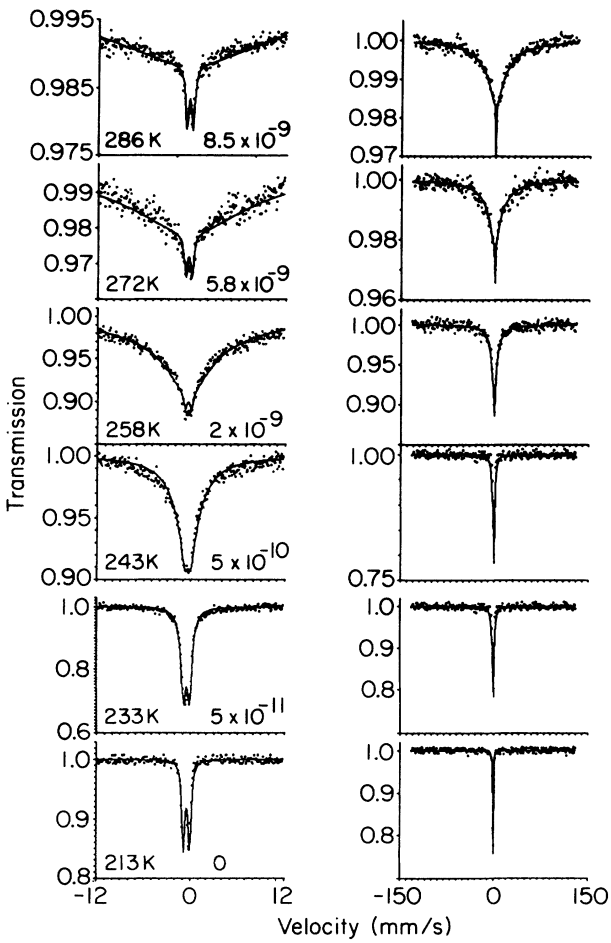

FIG. 1. Mössbauer spectra of sample 2 (2% cross-linkage) measured at different temperatures. Below 243 K the amount of material in the sample holder was reduced by a factor of 2 to avoid saturation effects. Solid lines represent the simulations of Eqs. (5) and (9). Left side: small velocity window, right side: large velocity window; numbers: temperature (K) and diffusion constant D (cm^2/s).

tions of fluctuation times.[40] The decrease of the area was shown to arise from the appearance of very broad, unresolvable lines. The supercooled sucrose-water solution within our polymer network will also give rise to similar broad components. An alternative explanation for the decreasing area is the influence of phonon modes of the network activated at about 250 K. Drying of the samples resulted in a complete disappearance of any spectral broadening at room temperature already at a water content smaller than 100 mg/g polymer and an increase (up to saturation) of the observed spectral area. The temperature dependence of the spectral area of the dehydrated sample shows the usual solidlike behavior (compare Fig. 4). After partial dehydration the dynamical properties of the samples are recovered by rehydration. These results support the assumption that the particles take part in the diffusion as a whole.

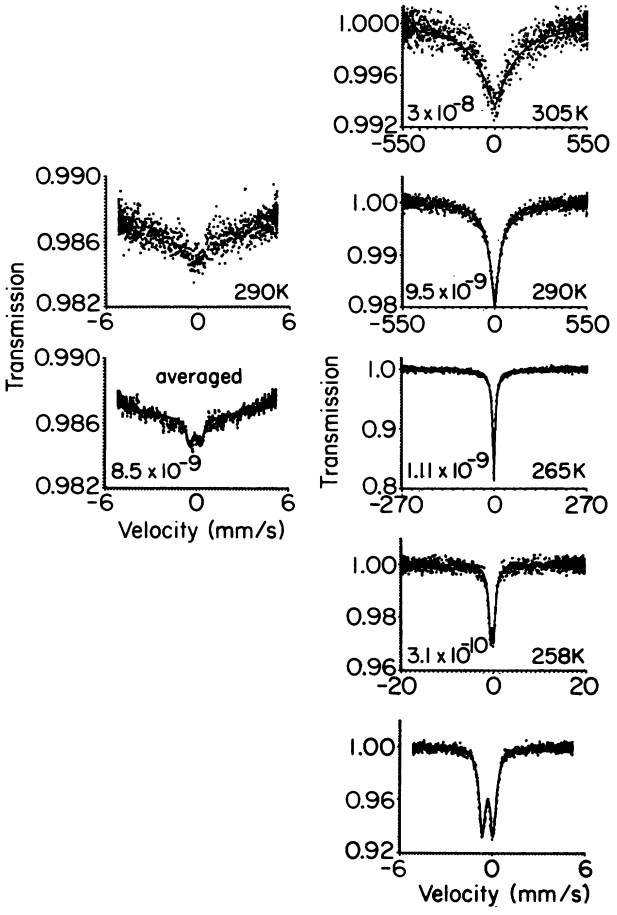

FIG. 2. Mössbauer spectra of sample 1 (1% cross-linkage). For low temperatures (251 and 258 K) a sample with natural Fe was used. Pay attention to the width of the spectral window which is increased from low-temperature to high-temperature spectra 100 times in order to see the full spectral width. For comparison, the limiting values of the diffusion coefficient, D, are given in cm^2/s. On the left side the central parts of the spectra are zoomed out. Even at 290 K the presence of a narrow component is clearly seen. Its fraction of the total area ia 0.0015.

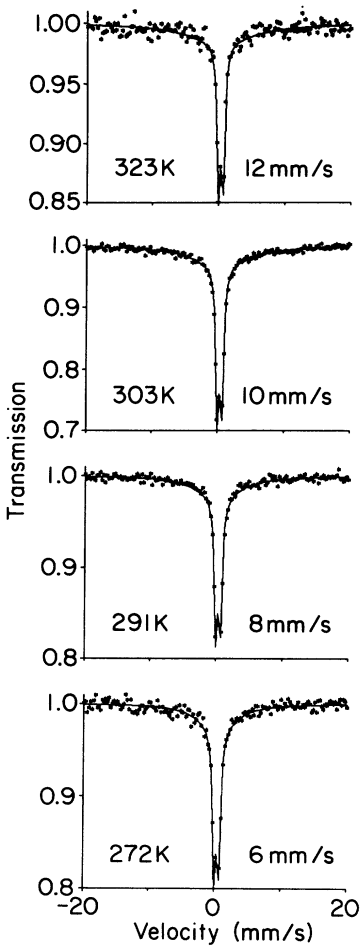

FIG. 3. Mössbauer spectra of sample 9 (12% cross-linkage). The data are fitted by a superposition of one narrow and one broadened component only. The temperatures (K) and the widths of the broad lines (mm/s) are given in the figure.

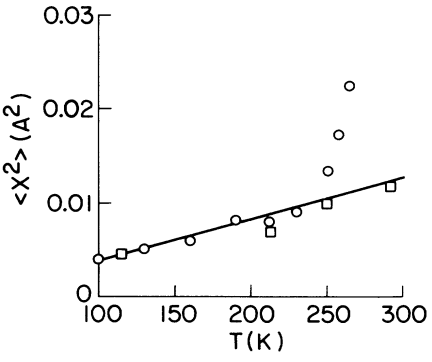

FIG. 4. Effective mean square displacements as determined from the temperature dependence of total spectral area, $\langle x^2\rangle = k^2 \ln A$, squares: dried sample; circles: sample 1 with natural iron. The areas are normalized so that the curves extrapolate to $\langle x^2\rangle = 0$ at $T = 0$ K.

For a theoretical treatment we start from the spectral function of a Mössbauer absorber:[1]

$$\phi(\omega)\sim \mathrm{Re}\int_0^\infty \exp\left[-i\omega t-\frac{\Gamma}{2}t\right] \times\langle \exp[i\mathbf{k}\cdot\mathbf{r}(0)-i\mathbf{k}\cdot\mathbf{r}(t)]\rangle dt \ . \quad (1)$$

Here, $\mathbf{r}(0)$ and $\mathbf{r}(t)$ are the coordinates of the center of mass of a particle at the time 0 and t, respectively. The Mössbauer radiation is characterized by the wave vector $\mathbf{k}$ and the lifetime Γ^{-1}. We consider the motion of the particles in an effective potential under the influence of stochastic forces yielding Brownian motion. Then the presence of phonon components will lead to a spectral area proportional to the Lamb-Mössbauer factor $f_a=\exp(-k^2\langle x^2\rangle)$. For the observables in the low-frequency Mössbauer window, $\mathbf{r}(t)$ in Eq. (1) can be treated as a classical stochastic process. Thus the quantum average may be substituted by a classical pair correlation function:

$$\langle\cdots\rangle=f_a(T)\int\int d\mathbf{r}_0 dr\, P_0(\mathbf{r}_0)P(\mathbf{r}_0,\mathbf{r},t) \times\exp[i\mathbf{k}\cdot(\mathbf{r}_0-\mathbf{r})] \ , \quad (2)$$

where P_0 is the initial probability for the ^{57}Fe nucleus to be at point $\mathbf{r}_0$; P is the probability of displacement to $\mathbf{r}$ in the time t. It is known that in case of diffusion in some arbitrary potential $U(\mathbf{r})$ in the overdamped (the most characteristic) regime, the trajectory of a probe obeys the Langevin equation:

$$\beta\dot{\mathbf{r}}=-\frac{\partial U(\mathbf{r})}{\partial\mathbf{r}}+F(t) \ , \quad (3)$$

where $\beta(T)$ is the friction coefficient and $F(t)$ characterizes white noise: $\langle F_i(t)F_j(t')\rangle=2T\delta_{ij}(t-t')$. (Here and below the temperature will be given in units of energy.) In this case the probability P in Eq. (2) obeys the diffusion Fokker-Planck equation:

$$\frac{\partial P}{\partial t}=D\left[\Delta P+\frac{1}{T}\frac{\partial U}{\partial\mathbf{r}}\frac{\partial P}{\partial\mathbf{r}}\right]=-\hat{R}P \ , \quad (4)$$

with the diffusion coefficient $D=T/\beta(T)$ and the initial condition $P(t=0)=\delta(\mathbf{r}-\mathbf{r}_0)$.

Here, the first term in the operator $\hat{R}$ corresponds to the homogeneous diffusion in the whole space while the second makes the particle move regularly towards the minima of the potential U. If there is no potential (free diffusion) the answer can be obtained immediately by inserting Eq. (3) into Eqs. (1) and (2) and the spectrum consists of a single Lorentzian with a broadening $\Delta\Gamma=2Dk^2$. In the general case, the Mössbauer spectrum of the particle can be represented as a sum of Lorentzians as was shown in Refs. 22 and 23:

$$\phi(\omega)\sim\sum_{n=0}^{\infty}\frac{A_n(\Gamma/2)+D\varepsilon_n)}{\omega^2+(\Gamma/2+D\varepsilon_n)^2} \ , \quad \sum_{n=0}^{\infty}A=1 \ . \quad (5)$$

Here, the weights A_n and the broadenings $D\varepsilon_n$ should be determined via the eigenstates and eigenvalues of an appropriate Fokker-Planck operator:

$$\hat{R}\psi_n=D\varepsilon_n\psi_n \ , \quad A_n=\left|\int d\mathbf{r}\exp(i\mathbf{k}\cdot\mathbf{r})\psi_n\right|^2 . \quad (6)$$

The main point is that one of the eigenvalues is always known; it is ε_0 corresponding to the state of thermal equilibrium:

$$\psi_0=\frac{1}{Z}\exp[-U(\mathbf{r})/T] \ , \quad Z=\int d\mathbf{r}\exp[-U(\mathbf{r})/T] \ . \quad (7)$$

It is clear that the corresponding narrow component should always be present in the spectra. Moreover, its weight can be derived directly from the profile of the potential:[23]

$$A_0=\frac{1}{Z^2}\left|\int\exp(i\mathbf{k}\cdot\mathbf{r})\exp(-U/T)d\mathbf{r}\right|^2 . \quad (8)$$

It is this relation that provides a clue for understanding the whole set of Mössbauer data. It is, however, essential that $A_0(T)$ be determined with a good precision.

From the spectra (Figs. 1–3) one can see that only for sample 2 the narrow component can be traced as a needlelike part of a spectrum up to the highest temperatures. Careful examination of the spectra shows that the weight of the narrow component is surprisingly constant: $A_0=0.017$. The lowest temperatures are not taken into account since the narrow component cannot be separated from the rest. A temperature-independent A_0 is possible only if in the whole temperature range $U=0$ inside of some cavity and infinite outside of it. In other words, to provide the observed constant value of A_0 the diffusion should proceed in the deep potential well with steep walls and flat bottom. The only variable changing with temperature is the diffusion coefficient.

For simplicity, let us consider the diffusion in a spherical cavity of radius r as a hole in the Swiss cheese. Fortunately in this case the Fokker-Planck equation can be solved exactly.[41] Its solution implies a double sum in (5) with indices n and 1 running from 0 to ∞ where

$$A_{ln}=\frac{6\mu_{ln}^2}{\mu_{ln}^2-l(l+1)}\left[\frac{krj_{l+1}(kr)-lj_l(kr)}{(kr)^2-\mu_{ln}^2}\right]^2 ; \quad l,n=0,\infty \quad (9)$$

$$A_\infty=\frac{9(\sin kr-kr\cos kr)^2}{(kr)^6} \ ; \quad \varepsilon_n=(\mu_{ln}/r)^2 \ .$$

μ_{ln} is the nth root of the transcendental equation $j_l(\mu)=0$ and $j(z)$ is a spherical Bessel function

$$j_l(z)=z^l\left[-\frac{1}{z}\frac{d}{dz}\right]^l\frac{\sin z}{z} \ . \quad (10)$$

In order to calculate the Mössbauer spectrum according to Eq. (5), we have to adjust the two parameters r and D. The parameter r enters via A_n and ε_n [compare Eqs. (9) and (10)]. It can be shown that a summation $n=1$ to 3 and $l=0$ to 5 is sufficient to describe all measured spectra.

First of all, we can deduce the value of the mean radius of a cage for sample 2; With $A_0=0.017$ and $kr=3.8$ we

obtain $r=0.5$ Å. Only the parameter D remains to be determined. A numerical fit using Eqs. (5)–(9) gives good results as shown in Fig. 1 by the solid line. The obtained D values are given in the figures. Note that slightly different diffusion constants D have to be used in the simulations in order to fit the whole velocity range of the spectra or only the low-velocity part. The temperature dependence of the diffusion coefficient is close to the Arrhenius law (Fig. 5). Also the strange behavior of the quadrupole doublet becomes clear: When the temperature is increased the higher Lorentzian spectral components become broadened but the narrow one is not yet resolved. As a result the full spectrum looks as if there were an overall broadening and the doublet collapses. As the widths of the broad Lorentzian become sufficiently larger than the natural linewidth, the narrow component can be resolved and the doublet can be seen again. Now its weight is A_0 and the rest of the area of the spectrum comes into the pedestal as can be seen in Fig. 1 for low velocities.

For the sample 2 the Mössbauer data give a self-consistent description of the motion of ferric hydroxide particles as a diffusion in a spherical cavity with a radius of 0.5 Å and reflecting walls. Note that this value corresponds to the displacements of the center of mass of the particle. So it is squeezed by the cavity rather tightly.

It should be emphasized that the successful procedure given above becomes possible only due to a fortunate combination of the values of A_0 and D allowing the precise determination of $A_0(T)$. For the sample 1 this procedure is not feasible because here A_0 cannot be extracted from the spectra so easily. Nevertheless, from our experience with sample 2, the type of potential is already known. Since the weaker cross-linkage corresponds to looser cages we may try to fit the spectra by the same model with a larger value of r. Indeed, for sample 1 we obtain good fits with $kr=4.8$ ($r=0.66$ Å). D follows again the Arrhenius law. At first glance it seems strange that an increase of the radius of the spherical cavity of only 0.16 Å explains the dramatic changes in the spectra passing from the spectra of sample 1 to 2. However, it should be taken into account that the amplitude of displacements in sample 2 is already comparable to the γ-ray wavelength. As a result, the situation is close to the free-diffusion limit and the highest weight corresponds to the Lorentzian component with a broadening of about $2Dk^2$. Any further increase in the size of the cage is felt by the nucleus as a step towards the free-diffusion limit. For sample 1 the spectra are almost fully transformed into a single broad line, especially at high temperatures. Nevertheless, even at these temperatures the spectra show the visible presence of a narrow line (compare the small velocity window in Fig. 2). Here is an example of how "free" diffusion can be seen in the solid matrix.

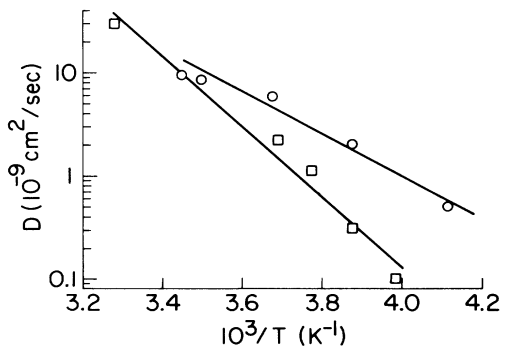

FIG. 5. Arrhenius plot of the diffusion coefficient D. The low-temperature points where the broadening is small in comparison with device linewidth are omitted. Squares: sample 1; circles: sample 2.

In the previous cases we considered a cavity with reflecting walls. Certainly it is an approximation of a real smooth confined potential with finite wall rigidity. In cases of the samples 1 and 2 this approach was reasonable since the region where U rises was much smaller than the cage. On the contrary, in case the cross-linkage is very tight, we can probe the steepness of the walls and thus the flexibility of the covalent network because the region of free diffusion should now be absent. Indeed, in sample 9 the displacements are very small and the spectrum consists of only two components—a narrow and a broad one. The temperature behavior shows that now the potential is in fact quadratic: $A_0=\exp(-k^2\langle r^2\rangle)$, $A_1=k^2\langle r^2\rangle\exp(-k^2\langle r^2\rangle)$ with the same values of D given in Figs. 1 and 2. The effective mean square displacements grow here very slowly due to the very steep potential. Even at room temperature $\sqrt{\langle r^2\rangle}=0.1$ Å. We then have $A_n<<1$ from $n=2$ on and the higher Lorentzians are negligible. So in our temperature range we are always in the domain where the spectra can be decomposed into one narrow and only one broadened spectral line. This decomposition gives the fit shown in Fig. 3 by a solid line. Thus $r\approx 0.1$ Å is a value characterizing the effective rigidity of covalent bonds with respect to the large particles at room temperature.

By varying the cross-linkage we have passed from free diffusion in the restricted volume to diffusion of the harmonic Brownian oscillator. Despite the fact that we have already changed the effective radius of the potential well and varied the diffusion coefficient by means of heating, there is one more independent way to study the behavior of the particles. The diffusion coefficient may be mediated not only via temperature but also by viscosity. For these experiments we used the substances prepared from samples 2 (cross-linkage 2%) and samples 6 (cross-linkage 4%). Only the viscosities of the solvating liquids were different. All spectra were measured at 290 K. In accordance with the initial assumption it should be equivalent to using different values of the diffusion coefficient. However, now there is no temperature variation, i.e., the shape of potential remains the same for all spectra. As can be seen in Fig. 6 for samples 6, the crossover from a viscous 60% sucrose solution to the case of pure water can be fully explained by the diffusion coefficient gradually decreasing by a factor of 3. In the case of pure water it is seen that the area of the narrow component represents only 8% of the whole spectrum while most of the area disappeared into the pedestal. The corresponding radius of the potential well is 0.48 Å and this value was kept

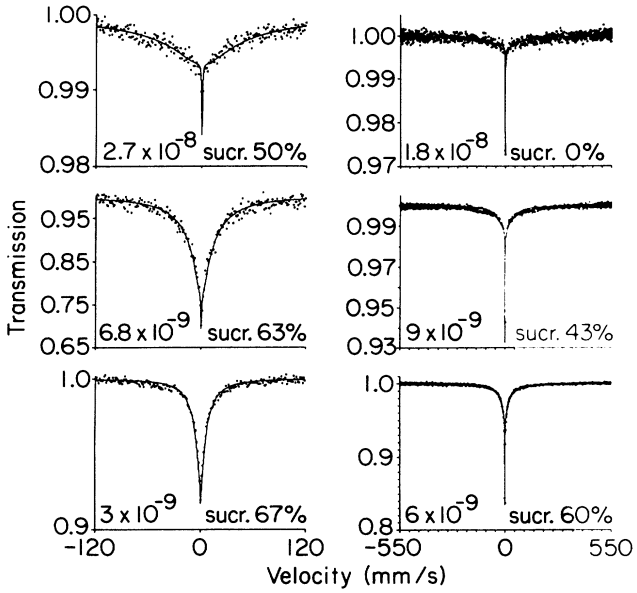

FIG. 6. Viscosity dependence of Mössbauer spectra of sample 2 (left side) (2% cross-linkage) and sample 6 (right side) (4% cross-linkage) at 290 K. Values of the diffusion coefficient D are given in cm^2/s. The different sucrose content is indicated.

constant in the spectral fitting for all viscosity. Pronounced changes of the spectral shape take place in samples 2–5 when the sucrose content is reduced from 67% to 50%. The radius of the potential well is $r=0.5$ Å, i.e., it is the same as in Fig. 1. The weight of the narrow line corresponds to $A_0=0.017$. We present the schematic plot of the potential as depicted in Fig. 7.

In conclusion, we have obtained a fully self-consistent description of diffusion in a polymer system covering a wide range of physical parameters. It seems that this approach can be successfully used also in a wider field of studies of porous systems and membranes.

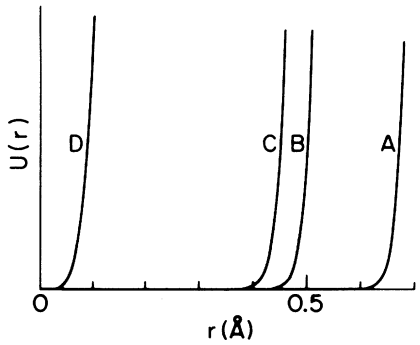

FIG. 7. Reconstruction of the effective potential for the ferric hydroxide particles in the polymeric network with different degrees of cross-linkage. Note that the coordinate r stands for the displacement of the center of mass of the particle while its radius is much larger.

ACKNOWLEDGMENTS

This work was carried out in the frame of a cooperation program supported by the Deutsche Forschungsgemeinschaft and the Academy of Sciences of the USSR. We acknowledge the support of the Kurchatov Institute of Atomic Energy, the Bundesministerium für Forschung und Technologie, the National Science Foundation, and the Fond der Chemie.

*Deceased.
†To whom correspondence should be addressed.
[1]K. S. Singwi and A. Sjolander, Phys. Rev. **120**, 1093 (1960).
[2]H. Keller and W. Kündig, Solid State Commun. **16**, 253 (1975).
[3]H. Winkler, H. J. Heinrich, and E. Gerdau, J. Phys. (Paris) Colloq. **37**, C6-261 (1976).
[4]R. C. Knauer and J. G. Mullen, Phys. Rev. **174**, 711 (1968).
[5]M. A. Krivoglaz and S. P. Repetskii, Fiz. Tverd. Tela (Leningrad) **8**, 2908 (1966) [Sov. Phys. Solid State **8**, 2325 (1967)].
[6]G. Vogl, W. Mansel, and P. H. Dederichs, Phys. Rev. Lett. **36**, 1497 (1976).
[7]W. Petry, G. Vogl, and W. Mansel, Phys. Rev. Lett. **45**, 1862 (1980).
[8]A. Bläsius, R. S. Preston, and U. Gonser, Z. Phys. Chem. Neue Folge **195**, 187 (1979).
[9]W. Petry and G. Vogl, Z. Phys. B **45**, 207 (1982).
[10]F. Parak and H. Formanek, Acta Crystallogr. **A27**, 573 (1971).
[11]F. Parak, E. N. Frolov, A. A. Kononenko, R. L. Mössbauer, V. I. Goldanskii, and A. B. Rubin, FEBS Letts. **117**, 368 (1980).
[12]H. Keller, and P. G. Debrunner, Phys. Rev. Lett. **45**, 68 (1980).
[13]I. Nowik, S. G. Cohen, E. R. Bauminger, and S. Ofer, Phys. Rev. Lett. **19**, 1528 (1983).
[14]E. W. Knapp, S. F. Fischer, and F. Parak, J. Chem. Phys. **78**, 4701 (1983).
[15]I. Nowik, E. R. Bauminger, S. G. Cohen, and S. Ofer, Phys. Rev. A **31**, 2291 (1985).
[16]Y. F. Krupyanski, F. Parak, V. I. Goldanskii, R. L. Mössbauer, E. Gaubmann, H. Engelmann, and I. P. Suzdalev, Z. Naturforsch. **37C**, 57 (1982).
[17]G. U. Nienhaus, H. Hartmann, F. Parak, J. Heinzl, and E. Huenges, Hyperfine Interact. **47**, 299 (1989).
[18]G. U. Nienhaus, J. Heinzl, E. Huenges, and F. Parak, Nature **338**, 665 (1989).
[19]H. Frauenfelder, F. Parak, and R. D. Young, Annu. Rev. Biophys. Biophys. Chem. **17**, 451 (1988).
[20]G. Vogl, Hyperfine Interact. **56**, 197 (1990).
[21]K. V. Shaitan and A. B. Rubin, Biofizika **25**, 796 (1980).
[22]W. Nadler and K. Schulten, Phys. Rev. Lett. **51**, 1712 (1983).
[23]A. M. Afanas'ev and V. E. Sedov, Phys. Status Solidi B **131**, 299 (1985).
[24]A. M. Afanas'ev, A. S. Plachinda, V. E. Sedov, V. I. Khromov, and L. V. Bashkeev, Khim. Fiz. **8**, 986 (1989).
[25]A. S. Plachinda, V. E. Sedov, V. I. Khromov, L. V. Bashkeev, and I. P. Suzdalev, Chem. Phys. Lett. **175**, 101 (1990).
[26]G. U. Nienhaus, A. S. Plachinda, M. Fischer, V. I. Khromov, F. Parak, I. P. Suzdalev, and V. I. Goldanskii, Hyperfine In-

teract. **56**, 1471 (1990).
[27]S. Plachinda, V. E. Sedov, V. I. Khromov, L. V. Bashkeev, and I. P. Suzdalev, Hyperfine Interact. **56**, 1483 (1990).
[28]A. A. van der Giessen, J. Inorg. Nucl. Chem. **28**, 2155 (1966).
[29]K. Kauffman and F. Hazel, J. Colloid Interface Sci. **51**, 422 (1975).
[30]J. Dousma and P. L. de Bruyn, J. Colloid Interface Sci. **64**, 154 (1978).
[31]P. J. Murphy, A. M. Posner, and J. P. Quirk, J. Colloid Interface Sci. **56**, 270 (1976); **56**, 284 (1976); **56**, 298 (1976); **56**, 312 (1976).
[32]J. M. D. Coey and P. W. Readman, Earth Planet Sci. Lett. **21**, 45 (1973).
[33]K. J. Atkinson, A. M. Posner, and J. P. Quirk, J. Inorg. Nucl. Chem. **30**, 2371 (1968).
[34]J. M. D. Coey and P. W. Readman, Nature **246**, 476 (1973).
[35]S. Orkamoto and H. Sekizawa, J. Phys. (Paris) Colloq. **40**, C2-137 (1979).
[36]K. M. Towe and W. F. Bradley, J. Colloid Interface Sci. **24**, 382 (1967).
[37]An-Yeng, C. F. Steve, G. Denes, E. Greezdan, R. Eaton, and F. Birchhall, Inorg. Chem. **23**, 1513 (1984).
[38]S. Morup, J. A. Dumesic, and H. Topsoe, in *Applications of Mössbauer Spectroscopy,* edited by R. L. Cohen (Academic, New York, 1980), Vol. 2, p. 1.
[39]These data were taken from J. Timmermans, *The Physicochemical Constants of Binary Systems in Concentrated Solutions* (Interscience, New York, 1960), Vol. 4, p. 309.
[40]G. U. Nienhaus, H. Frauenfelder, and F. Parak, Phys. Rev. B **43**, 3345 (1991).
[41]F. Volino and A. J. Dianoux, Mol. Phys. **41**, 271 (1980).